Journal of Mathematical Chemistry 19 (1996) 241–263 

# Specification of chirality for links and knots

Chengzhi Liang, Corinne Cerf and Kurt Mislow

*Department of Chemistry, Princeton University, Princeton, NJ 08544, USA*

Received 26 February 1996

A general scheme has been developed for the assignment of chirality descriptors to chiral links and knots. For oriented links and knots, the new D/L scheme employs linking numbers, self-writhes, and writhe profiles, in descending hierarchical order, with self-writhes and writhe profiles limited to alternating links and knots. A related scheme applies to non-oriented links and knots. In a modification of a previous scheme, the use of vertex-bicolored digraphs is introduced in order to compute writhe profiles of oriented links and knots. It is pointed out that even though the different geometric presentations of each individual chiral knot or link can be partitioned into homochirality classes, the links and knots that belong to a given configurational class, D or L, are not homochirally similar.

## 1. Introduction

We recently reported a scheme for assigning chirality descriptors (D and L) to topologically chiral knots [1]. In the course of a subsequent study of topologically chiral and achiral links [2], the question arose whether a method could be found to effect a similar classification of chiral links. Our goal was to develop a unified scheme that would encompass knots as well as links; a unified scheme is desirable because a knot is just a special case of a link, i.e., a link with only one component. The present paper describes a general scheme that incorporates this desirable feature. As will become clear in what is to follow, this process of unification entails an extensive revision of our previous scheme [1].

In order to consider all possible topological constructions of links and knots, account must be taken of orientation and invertibility [3]. In general, any given diagram $D(K)$ of a non-oriented link $K$ with $m$ components upon orientation yields a set of $2^m$ oriented diagrams $D^l(K^l)$. Equivalences or non-equivalences among these diagrams depend on geometric or topological relationships. In the case of knots ($m = 1$), the two oriented diagrams are topologically equivalent if the knot is invertible (e.g., $3_1$) and non-equivalent if it is non-invertible (e.g., $8_{17}$). The situation becomes significantly more complex in links with $m > 1$, as illustrated in Figs. 1–5 for the case of alternating links with $m = 2$. The notation is that of Doll and Hoste [4], in which the components are indexed numerically and the orientation of each component is symbolized by a "+" or "−" sign.

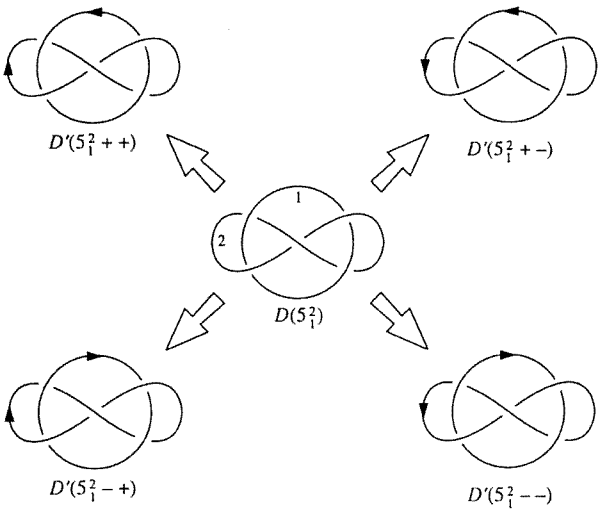


Fig. 1. The four oriented diagrams derived from the minimal-crossing diagram of one enantiomorph of the link $5_1^2$. $D'(5_1^2++) = D'(5_1^2--) = D'(5_1^2+-) = D'(5_1^2-+)$.

In the simplest case, illustrated by one enantiomorph of the non-oriented Whitehead link, $5_1^2$ (Fig. 1), the four oriented diagrams are all related by twofold rotations in 3-space, so there is only one isotopy type. This can be represented by a

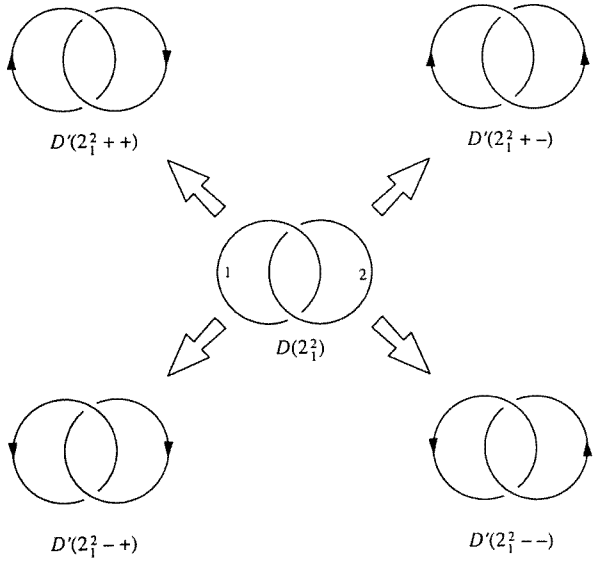


Fig. 2. The four oriented diagrams derived from the minimal-crossing diagram of the amphicheiral link $2_1^2$. $D'(2_1^2++) = D'(2_1^2--) \neq D'(2_1^2+-) = D'(2_1^2-+)$. $D'(2_1^2++)$ and $D'(2_1^2+-)$ are topological enantiomorphs.

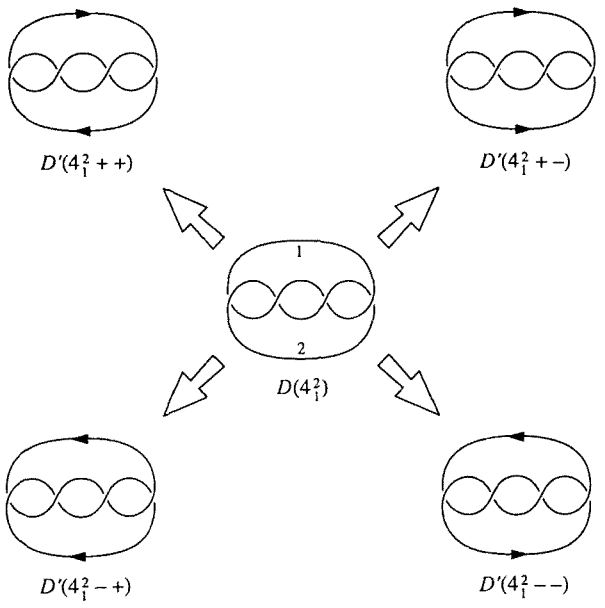


Fig. 3. The four oriented diagrams derived from the minimal-crossing diagram of one enantiomorph of the link $4_1^2$. $D'(4_1^2++) = D'(4_1^2--) \neq D'(4_1^2+-) = D'(4_1^2-+)$. $D'(4_1^2++)$ and $D'(4_1^2+-)$ are topological diastereomorphs.

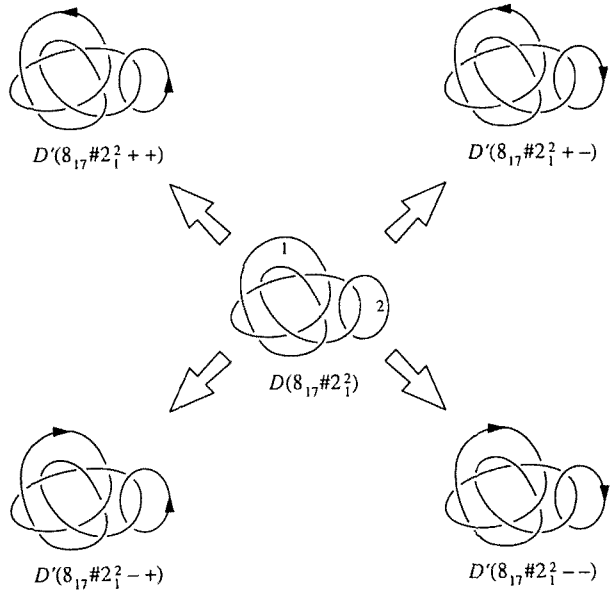


Fig. 4. The four oriented diagrams derived from the minimal-crossing diagram of the amphicheiral link $8_{17}\#2_1^2$. They represent four different isotopy types, with the relationships: $D'(8_{17}\#2_1^2++) = D'(8_{17}\#2_1^2+-)^*$, $D'(8_{17}\#2_1^2--) = D'(8_{17}\#2_1^2-+)^*$ [A "*" symbol denotes the mirror image].

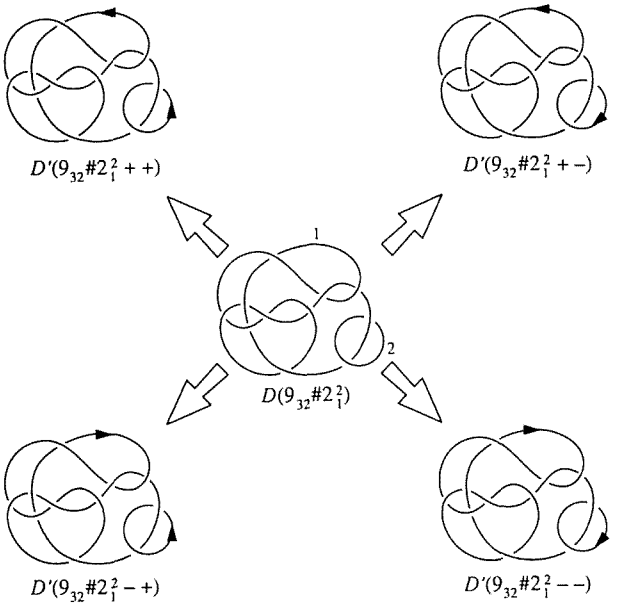


Fig. 5. The four oriented diagrams derived from the minimal-crossing diagram of one enantiomorph of the link $9_{32}\#2_1^2$. They represent four topological diastereomorphs.

single diagram, say $D'(5_1^2++)$. In the second case, illustrated by the amphicheiral non-oriented Hopf link, $2_1^2$ (Fig. 2), the four oriented diagrams are pairwise related by twofold rotations in 3-space, i.e., $2_1^2++$ and $2_1^2--$; $2_1^2+-$ and $2_1^2-+$. Because of the amphicheirality of the non-oriented link, the resulting two isotopy types are related as enantiomorphs that can be represented by two oriented diagrams, say $D'(2_1^2++)$ and $D'(2_1^2+-)$. In the third case, illustrated by one enantiomorph of the simplest topologically chiral non-oriented link, $4_1^2$ (Fig. 3), the four oriented diagrams are pairwise related by twofold rotations in 3-space, i.e., $4_1^2++$ and $4_1^2--$; $4_1^2+-$ and $4_1^2-+$. The resulting two isotopy types are *not*, however, related as enantiomorphs since the non-oriented link is chiral. We refer to them as diastereomorphs. The two diastereomorphs can be represented by two oriented diagrams, say $D'(4_1^2++)$ and $D'(4_1^2+-)$.

In the three cases listed thus far, both components are invertible knots. In the remaining two cases, one or both components are non-invertible. In the first case, both non-oriented components are amphicheiral. This case is illustrated by $8_{17}\#2_1^2$ (Fig. 4), an amphicheiral composite link one of whose components ($8_{17}$) is non-invertible. Orientation now yields four isotopy types, two diastereomorphs, i.e., $8_{17}\#2_1^2++$ and $8_{17}\#2_1^2+-$, and their respective enantiomorphs, i.e., $8_{17}\#2_1^2--$ and $8_{17}\#2_1^2-+$. The four types may be represented by the four oriented diagrams in Fig. 4. In the second case, one or both non-oriented components are chiral. This case is illustrated by one enantiomorph of the composite link $9_{32}\#2_1^2$ (Fig. 5), a chiral composite link one of whose components ($9_{32}$) is non-invertible. Again,

orientation yields four isotopy types, but now all four are diastereomorphs. The four types may be represented by the four oriented diagrams in Fig. 5.

## 2. Oriented links and knots

The assignment of D and L configurations to chiral oriented links and knots follows the flowchart in Fig. 6. The first step consists in determining the linking number. Given an oriented link $K'$, the linking number $l(K')$ is one half the sum of the characteristics $\epsilon$ (i.e., the crossing number $+1$ or $-1$ in Fig. 1.34 of [5]) of the inter-component crossings. The linking number is an invariant of $K'$ [5]; that is, $l(K')$ remains unchanged under ambient isotopies. If $l(K') \neq 0$, then the sign of $l(K')$

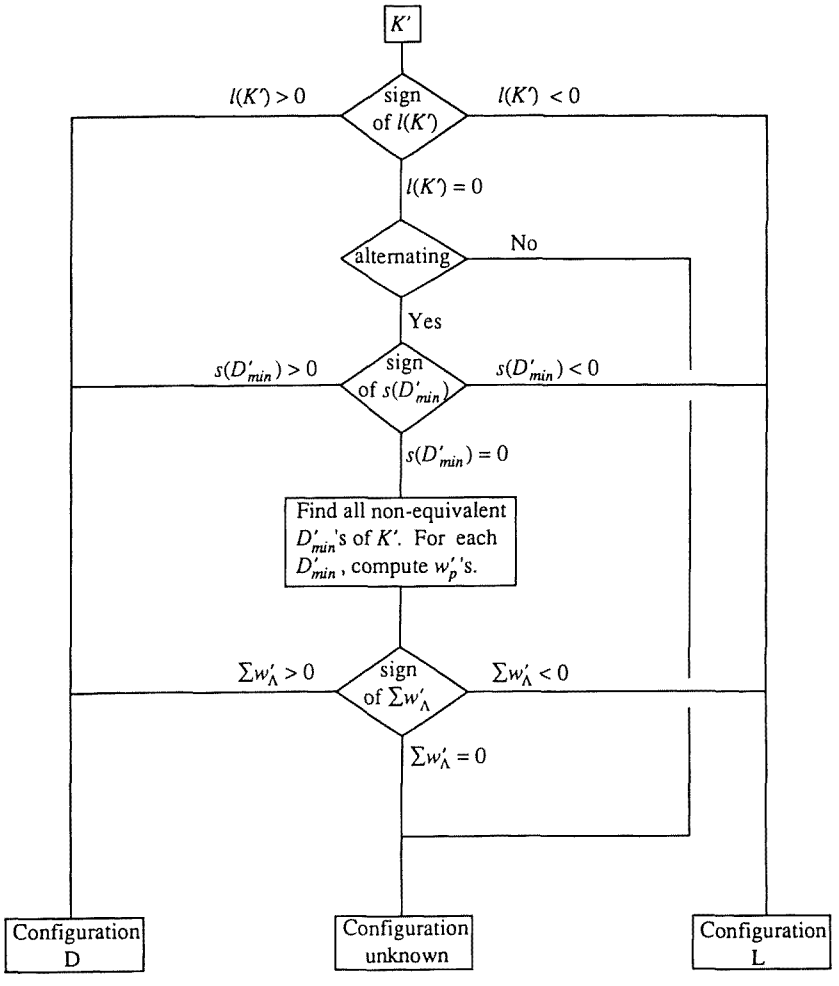


Fig. 6. Flowchart for the D/L specification of a given oriented chiral link or knot $K'$.

determines the configuration of the link: the link is denoted D if $l(K') > 0$ and L if $l(K') < 0$. For example, $D'(2_1^2 + +)$ and $D'(2_1^2 + -)$ (Fig. 2) with $l(K') = +1$ and $-1$ have D and L configurations, respectively.

The linking number of all knots and of some links (e.g., $5_1^2$) is zero. Because a zero value of $l(K')$ cannot be used to assign configurations, we are forced to choose another descriptor: the self-writhe [8].

Let $D'_{min}$ denote a minimal-crossing diagram of $K'$. The writhe $w(D'_{min})$ is the sum of all the characteristics in $D'_{min}$. The $w(D'_{min})$ of an oriented alternating link is an invariant [6,7]. In other words, any two minimal-crossing diagrams of an oriented alternating link have the same $w(D'_{min})$.

Writhe $w(D'_{min})$ and linking number $l(D'_{min})$ satisfy the following relation:

$$w(D'_{min}) = s(D'_{min}) + 2l(D'_{min}), \tag{1}$$

where $s(D'_{min})$, the self-writhe, is the sum of the characteristics of self-crossings in components of $D'_{min}$. Because $w(D'_{min})$ and $l(D'_{min})$ are both invariants, it follows that $s(D'_{min})$ is also an invariant. The invariance of $s(D'_{min})$ is limited, however, to alternating links or knots, and no configurations can therefore be assigned to non-alternating knots, e.g., $8_{19}+$, or links, e.g., $8_{15}^2 + +$. For alternating links and knots, however, the sign of $s(D'_{min})$ determines the configuration of the link: the link is denoted D if $s(D'_{min}) > 0$ and L if $s(D'_{min}) < 0$. For example, all four oriented diagrams in Fig. 1 have $l(K') = 0$ and $s(D'_{min}) = -1$, and hence correspond to the L configuration of the oriented Whitehead link. Similarly, the knot obtained by orientation of $3_1$ in Rolfsen's tabulation [9] has $l(K') = 0$ and $s(D'_{min}) = -3$ and hence is assigned the L configuration.

A zero value of $s(D'_{min})$ cannot be used to assign configurations. To classify oriented chiral links or knots with $l(D'_{min}) = 0$ and $s(D'_{min}) = 0$ (and therefore with $w(D'_{min}) = 0$) into D and L classes, another method must therefore be used. The approach that we have taken to specify the chirality of members in this "zero set" is based on the one developed previously for non-oriented knots [1].

At the heart of this method, called method of writhe profiles, is the transformation of a knot diagram into a vertex-bicolored graph by conversion of the crossing points and arcs of the diagram into the vertices and edges of the corresponding graph; over- and undercrossings are represented by appropriate (black or white) colors. The method of writhe profiles was designed to take advantage of the differences between the environments of black and white vertices in vertex-bicolored graphs that correspond to $D_{min}$'s of chiral knots. The difference is that we are now dealing with *oriented* links and knots, whose diagrams transform into *directed* graphs or digraphs, i.e., graphs with oriented arcs instead of edges. Note that while there is always a one-to-one mapping of oriented diagrams to vertex-bicolored *digraphs*, there is, in general, a many-to-one mapping of such diagrams to vertex-bicolored but non-oriented graphs; for example, $D'(4_1^2 + +)$ and $D'(4_1^2 + -)^*$ are represented by the same vertex-bicolored non-oriented graph.

As a first step, a diagram is constructed from the vertex-bicolored digraph; this diagram consists of a set of concentric spherical shells $S_p, p = 0, 1, 2, \ldots$, with vertex $i$ at the center ($p = 0$). Adjacent vertices are then placed on the nearest shell, $S_1$, and connected to vertex $i$. This process is continued in an outward direction, from $S_1$ to $S_2$, and so forth. In the present case, because digraphs are being used, vertex $j$ is said to be adjacent to vertex $i$ only if the vertices are connected by an arc directed from $i$ to $j$. The distinction between single and parallel double arcs is ignored; that is, even if there are two arcs directed from one vertex to another in the link digraph, these vertices will be connected by only one arc in the concentric-shell diagram.

Fig. 7 illustrates the construction of such a concentric-shell diagram from the vertex-bicolored digraph of the oriented knot $7_6+$. The resulting diagram differs significantly from the corresponding diagram constructed from the vertex-bicolored graph of the non-oriented knot (Fig. 4 in [1], with double edges replaced by single edges).

The $p$th order characteristic $\epsilon_{i(p)}$ of the $i$th vertex is then defined as the sum of the zeroeth-order characteristics of all the vertices $j_p$ on $S_p$ by eq. (2), where $p$ is the length of the walk from $i$ to $j_p$ in which the same vertices can be revisited without limit.

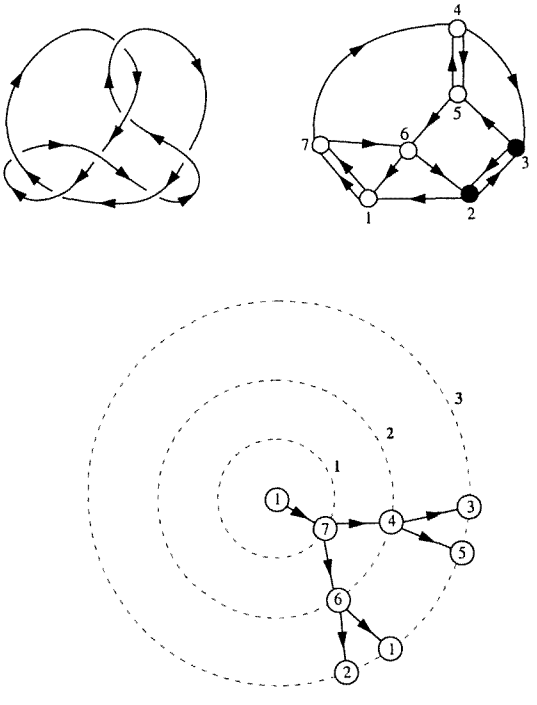


Fig. 7. Top left: Minimal-crossing diagram of oriented knot $7_6+$. Top right: The corresponding vertex-bicolored digraph with numbered vertices. Bottom: A concentric-shell diagram showing three $p$th order environments (bold-faced numbers) of vertex 1 at the center ($p = 0$).

$$\epsilon_{i(p)} = \sum_{j_p} \epsilon_{j_p(0)}\,, \quad p = 0, 1, 2, 3, \ldots\,. \tag{2}$$

In general, the distributive form of $\epsilon_{i(p)}$ over the $N$ characteristics is

$$\epsilon_{i(p)} = \sum_{k=1}^{N} r_{k,i(p)} \epsilon_{k(0)}\,, \quad p = 0, 1, 2, 3, \ldots\,, \tag{3}$$

where $r_{k,i(p)}$ is the contribution (or coefficient) of vertex $k$ to $\epsilon_{i(p)}$.

The $p$th-order writhe $w'_p$ is defined as the sum of the $\epsilon_{i(p)}$'s of all $N$ crossing points in the link diagram, i.e. of all $N$ vertices in the vertex-bicolored digraph. We introduce the "prime" symbol in order to remind the reader that we are dealing with oriented links:

$$w'_p = \sum_{i=1}^{N} \epsilon_{i(p)}\,, \quad p = 0, 1, 2, 3, \ldots\,. \tag{4}$$

The writhe profile of a diagram consists of a series of ordered writhes, $w'_0$, $w'_1$, $w'_2$, ... whose first member, $w'_0$ (the zeroeth-order writhe), represents $w(D'_{min})$. Note that for the zero set, $w(D'_{min}) = 0$, by definition.

Let us analyze the $w'_p$'s and their components $\epsilon_{i(p)}$, for $p$ running from zero to infinity. At $p = 0$, each $\epsilon_{i(0)}$ is either $+1$ or $-1$. Since the sum of the $\epsilon_{i(0)}$'s, $w'_0$, is equal to 0 for the zero set, half of the $\epsilon_{i(0)}$'s are $+1$ and half of them are $-1$. As the order $p$ increases, progressively more and more $\epsilon_{i(p)}$'s share the same sign until a given order, called $p_{min}$, is reached where all $\epsilon_{i(p)}$'s $\geqslant 0$ or all $\epsilon_{i(p)}$'s $\leqslant 0$. As was previously observed for non-oriented knots [1], in general there exists for every knot or link a $p_{min}$ such that all $\epsilon_{i(p)}$ components of $w'_p$ bear the same sign for $p \geqslant p_{min}$. Obviously, $p_{min} = 0$ if and only if all $\epsilon_{i(0)}$'s have the same sign, $+1$ or $-1$. We made the empirical observation that, starting with $p_{min}$, the absolute magnitude of the sum of $\epsilon_{i(p)}$'s, $w'_p$, increases monotonically with an increase in $p$ while its sign remains the same. This allows an unequivocal assignment of a sign, positive or negative, to the writhe profile, and overcomes the problem that the increase of $w'_p$ with an increase in $p$ may not necessarily be monotonic for $p < p_{min}$. Such erratic behavior had previously been observed for writhe profiles of the non-oriented knots $7_7$ and $9_{42}$ [1]. At that time this "$7_7$ syndrome" was thought to be rare, but we have since found that it is far from uncommon, at least among oriented knots and links. In the present work, however, we are only concerned with the $w'_p$'s of a link or knot diagram with $p \geqslant p_{min}$, and the $7_7$ syndrome, even when it does occur, therefore becomes irrelevant for our present purposes.

Another problem arises from the fact that the $D'_{min}$'s of links and knots are not topological invariants. Furthermore, the profiles are generally different for different $D'_{min}$'s of the same link or knot. For alternating links or knots, we can overcome this problem by generating all possible $D'_{min}$'s by the use of flypes [4,10,11]. As conjectured by Tait [10], and as proved by Menasco and Thistlethwaite [12], all possible

reduced diagrams of an alternating link or knot can be generated by operating with flypes on any reduced diagram. The same applies to $D'_{min}$'s, since it was proved that $D'_{min}$'s of alternating links and knots are also reduced [6]. Thus, with respect to alternating links and knots, the way is clear to find all $D'_{min}$'s.

First, how many $D'_{min}$'s are there? Fig. 8 depicts the graph of a generalized flyping diagram. The graph contains $v$ contiguous vertices followed by $t$ contiguous tangles T, where $T_1$ contains more than one vertex. Through flypes, each crossing can be "moved" to each inter-tangle space. The number $n(v, t)$ of $D'_{min}$'s that can be derived from this flyping graph, including the original graph, is given by the combinatorial expression

$$n(v,t) = \sum_{k=0}^{v} \frac{(k+t-2)!}{k!(t-2)!} . \tag{5}$$

Eq. (5) implies that $t \geqslant 2$, since flyping diagrams with only one tangle T give rise only to trivial flypes.

Several flyping diagrams can be generated from a given link diagram, depending on the crossing chosen to be "moved". The total number $n_{tot}(K')$ of $D'_{min}$'s of a link $K'$ is therefore given by

$$n_{tot}(K') = \prod_{i=1}^{z} n(v_i, t_i) = \prod_{i=1}^{z} \sum_{k=0}^{v_i} \frac{(k+t_i-2)!}{k!(t_i-2)!} , \tag{6}$$

where $z$ is the number of different flyping diagrams. All the $D'_{min}$'s of a given alternating knot or link can thus be exhausively enumerated.

It remains to determine the number of non-equivalent diagrams among those $n_{tot}(K')$ diagrams. Diagrams are said to be non-equivalent/equivalent if the corresponding vertex-bicolored digraphs are non-equivalent/equivalent. We denote the total number of non-equivalent $D'_{min}$'s of an oriented link or knot $K'$ by $n_{neq}(K')$.

For a given oriented link or knot, we are thus left with $n_{neq}(K')$ diagrams, for each of which we compute the writhe profile and determine its $p_{min}$. We then sum these profiles, order by order. As we are concerned only with the $w'_p$'s of a diagram with $p \geqslant p_{min}$, the $p_{min}$ of the sum of the profiles equals the largest $p_{min}$ among the summands. We denote this $p_{min}$ by $\lambda$ and define a new profile by the series

$$\sum_{n=1}^{n_{neq}} [w'_\lambda]_n, \sum_{n=1}^{n_{neq}} [w'_{\lambda+1}]_n, \sum_{n=1}^{n_{neq}} [w'_{\lambda+2}]_n, \ldots .$$

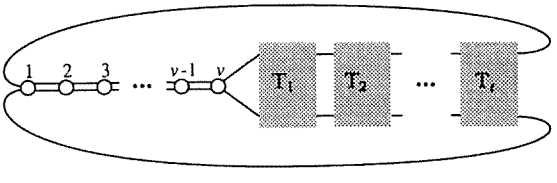


Fig. 8. Generalized flyping graph.

The configuration, D or L, of the oriented link or knot is determined by the sign of the first nonzero member of the series, $\sum w'_\Lambda$: D if $\sum w'_\Lambda$ is positive and L if it is negative. Results for links and knots in the zero set are summarized below.

Among oriented chiral alternating prime links with up to 9 crossings and 4 components [4], only five belong to the zero set (Fig. 9). Their configurations are listed in Table 1. For all but one of the five links, $n_{neq}(K') = 1$; the exception is $8^2_{10}++$ with $n_{neq}(K') = 4$. Note, with respect to Table 1, that oriented link $8^2_{10}$ has only one isotopy type, which means that all orientations are topologically equivalent. We arbitrarily call this oriented link $8^2_{10}++$. Links $8^3_1+-+$, $8^3_2+--$, $8^4_1+++-$, and $8^4_1++--$ are all invertible because of symmetry. They are therefore topologically equivalent to the oriented links with all components reversed. Again, we arbitrarily choose the names beginning with a "+" (e.g., $8^3_1+-+$ instead of $8^3_1-+-$).

The results for all oriented chiral alternating prime knots in the zero set with up to 10 crossings are combined in Table 2. The subset headed by $8_4+$ consists of invertible knots whose two orientations are equivalent. The orientation is arbitrarily denoted as "+". The subset headed by $8_{17}+(-)$ (Fig. 10) consists of noninvertible knots that are amphicheiral in their non-oriented state. The two oriented knots, $8_{17}+$ and $8_{17}-$, are therefore topological enantiomorphs whose configurations are necessarily opposite. The subset headed by $10_{91}+(-)$ (Fig. 10) consists of noninvertible knots that are chiral in their non-oriented state. The pairs of oriented knots in this subset are topological diastereomorphs; configurations of diastereomorphs are not related by symmetry and may therefore be either opposite or the same, as observed.

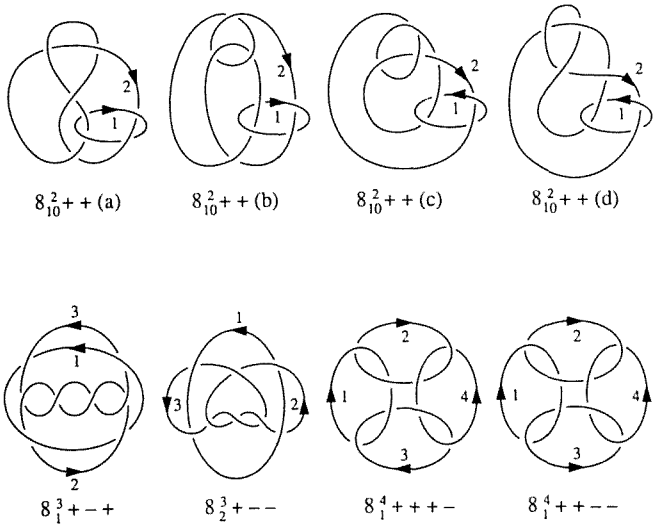


Fig. 9. Minimal-crossing diagrams of oriented chiral alternating links $8^2_{10}++$, $8^3_1+-+$, $8^3_2+--$, $8^4_1+++-$, and $8^4_1++--$. Labeling and orientation of components follow the convention in [4].

Table 1
Writhe profiles and configurations of all oriented chiral alternating prime links with up to 9 crossings and 4 components, and with $l(K')$ and $s(D'_{min}) = 0$ (Fig. 9) [a].

| Link diagram | $p_{min}$ | $w'_\lambda$ | $w'_{\lambda+1}$ | $w'_{\lambda+2}$ | $w'_{\lambda+3}$ | D/L |
|---|---|---|---|---|---|---|
| $8^2_{10}++$(a)[b] | 7 | +1475 | +2720 | +5025 | +9280 | |
| $8^2_{10}++$(b) | 5 | +2995 | +5492 | +10119 | +18600 | |
| $8^2_{10}++$(c) | 5 | +1140 | +2116 | +3920 | +7268 | |
| $8^2_{10}++$(d) | 13 | +163 | +288 | +551 | +1008 | |
| **$8^2_{10}++$** | **13(λ)** | **+5773** | **+10616** | **+19615** | **+36156** | **D** |
| **$8^3_1+-+$** | **4(λ)** | **+18** | **+34** | **+62** | **+110** | **D** |
| **$8^3_2+--$** | **17(λ)** | **−21** | **−30** | **−39** | **−52** | **L** |
| **$8^4_1++++-$** | **2(λ)** | **+4** | **+6** | **+12** | **+18** | **D** |
| **$8^4_1+++--$** | **8(λ)** | **+20** | **+28** | **+52** | **+92** | **D** |

[a] For each link, the line corresponding to $\sum w'_\lambda, \sum w'_{\lambda+1}, \ldots$ is indicated in boldface.
[b] Doll and Hoste [4] list this diagram as the only $D'_{min}$ of link $8^2_{10}++$.

Table 2
Configurations of all oriented chiral alternating prime knots with up to 10 crossings and with $w(D'_{min}) = 0$.

| Knot | $n_{neq}$ | λ | D/L |
|---|---|---|---|
| $8_4+$ | 1 | 3 | D |
| $10_{15}+$ | 4 | 8 | L |
| $10_{19}+$ | 4 | 4 | D |
| $10_{31}+$ | 8 | 10 | D |
| $10_{42}+$ | 24 | 11 | D |
| $10_{48}+$ | 2 | 25 | D |
| $10_{52}+$ | 4 | 5 | L |
| $10_{54}+$ | 4 | 5 | L |
| $10_{71}+$ | 18 | 15 | D |
| $10_{104}+$ | 1 | 31 | D |
| $10_{108}+$ | 1 | 5 | L |
| $8_{17}+(-)$ | 1 | 24 | L(D) |
| $10_{79}+(-)$ | 1 | 46 | L(D) |
| $10_{81}+(-)$ | 4 | 8 | L(D) |
| $10_{88}+(-)$ | 4 | – | unknown |
| $10_{109}+(-)$ | 1 | 28 | L(D) |
| $10_{115}+(-)$ | 1 | – | unknown |
| $10_{118}+(-)$ | 1 | 42 | L(D) |
| $10_{91}+(-)$ | 1 | 20(26) | D(L) |
| $10_{93}+(-)$ | 1 | 4(5) | D(D) |
| $10_{107}+(-)$ | 2 | 8(9) | D(D) |

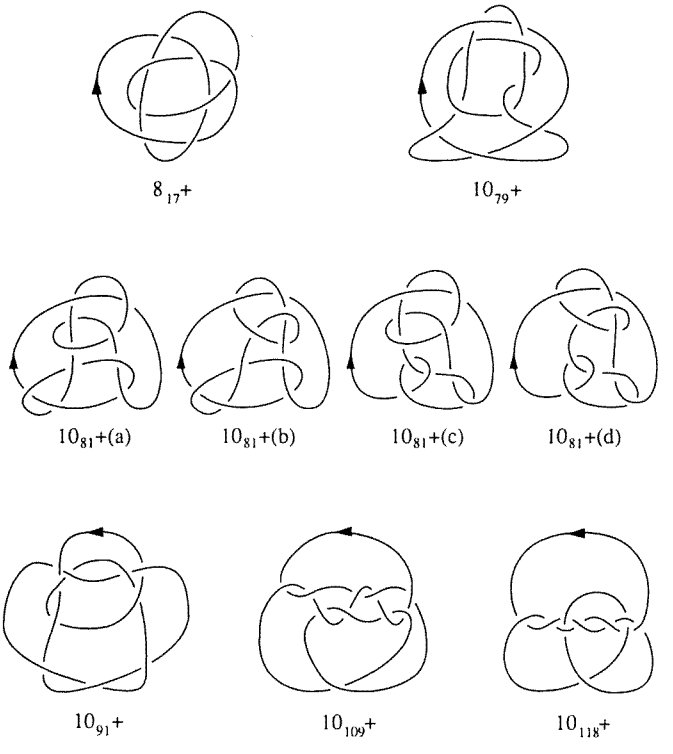


Fig. 10. Minimal-crossing diagrams of oriented chiral alternating knots $8_{17}+$, $10_{79}+$, $10_{81}+$, $10_{91}+$, $10_{109}+$, and $10_{118}+$.

With the exception of the three knots $10_{48}+$ (Fig. 11), $10_{71}+$ (Fig. 11), and $10_{81}+$ (Fig. 10), the writhe profiles of all the diagrams of a given knot in Table 2 were found to have the same sign. As shown in Table 3, the profiles of different diagrams in each of these three knots were found to be oppositely signed, but, thanks to the scheme described above, their configurations could nevertheless be unambiguously established.

No configurations could be assigned to oriented knots $10_{88}$ and $10_{115}$ because all the $w'_p$'s in their writhe profiles are zero. This peculiar result can be explained as follows. Recall that for any vertex $v$ of a digraph, its out-degree, $q_{out}(v)$, is the number of arrows pointing away from $v$, and its in-degree, $q_{in}(v)$, is the number of arrows pointing towards $v$ [13].

THEOREM

If a vertex-bicolored digraph is regular of degree $q$ ($q = q_{out} = q_{in}$), then its $p$th-order writhe $w'_p$ satisfies

$$w'_p = w'_0 q^p , \quad p = 0, 1, 2, 3, \ldots . \tag{7}$$

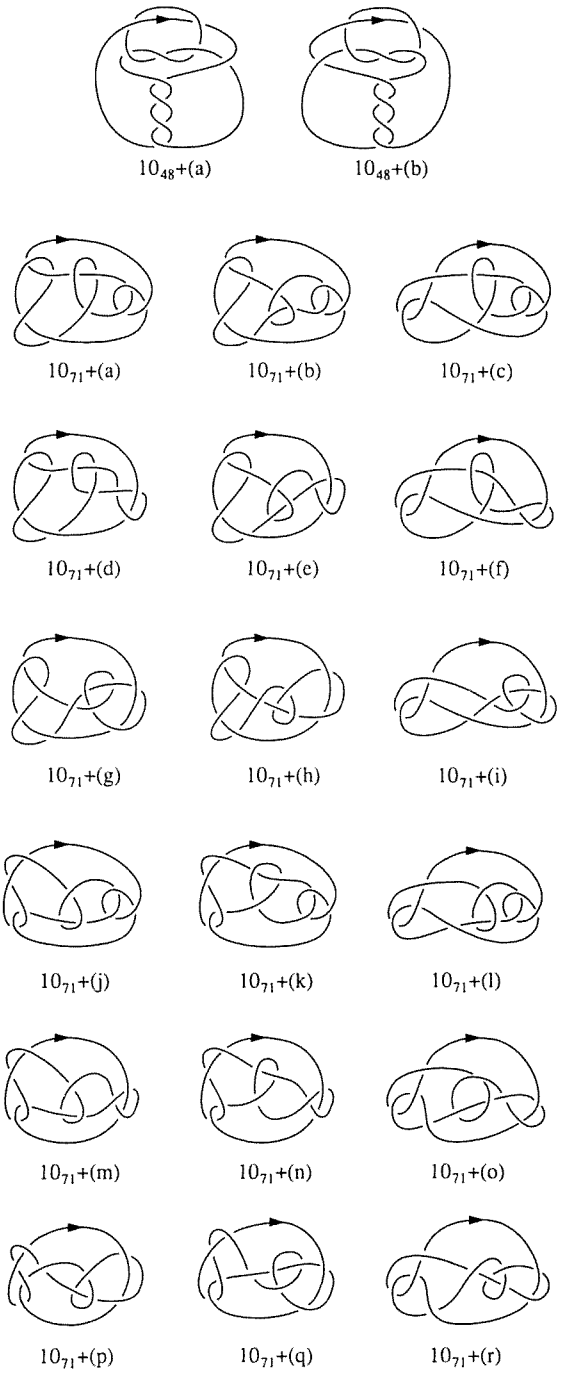


Fig. 11. Minimal-crossing diagrams of oriented chiral alternating knots $10_{48}+$ and $10_{71}+$.

Table 3
Writhe profiles and configurations of three selected oriented knots [a].

| Knot diagram | $p_{min}$ | $w'_{\lambda}$ | $w'_{\lambda+1}$ | $w'_{\lambda+2}$ | $w'_{\lambda+3}$ | D/L |
|---|---|---|---|---|---|---|
| $10_{48}+$(a) | 18 | +233 | +313 | +413 | +544 | |
| $10_{48}+$(b) | 25 | −45 | −59 | −79 | −106 | |
| **$10_{48}+$** | **25(λ)** | **+188** | **+254** | **+334** | **+438** | **D** |
| $10_{71}+$(a) | 11 | +535 | +969 | +1723 | +3112 | |
| $10_{71}+$(b) | 15 | −370 | −665 | −1230 | −2167 | |
| $10_{71}+$(c) | 9 | +5397 | +9890 | +17822 | +32315 | |
| $10_{71}+$(d) | 10 | +1774 | +3105 | +5542 | +9813 | |
| $10_{71}+$(e) | 6 | +2381 | +4219 | +7493 | +13323 | |
| $10_{71}+$(f) | 9 | +3866 | +6924 | +12389 | +22242 | |
| $10_{71}+$(g) | 7 | +7484 | +13498 | +24350 | +43885 | |
| $10_{71}+$(h) | 5 | +7270 | +13088 | +23560 | +42391 | |
| $10_{71}+$(i) | 10 | +8581 | +15576 | +28421 | +51734 | |
| $10_{71}+$(j) | 12 | +621 | +1119 | +2031 | +3600 | |
| $10_{71}+$(k) | 7 | +3222 | +5823 | +10482 | +18797 | |
| $10_{71}+$(l) | 6 | +3847 | +6986 | +12734 | +22985 | |
| $10_{71}+$(m) | 11 | −1552 | −2779 | −4916 | −8649 | |
| $10_{71}+$(n) | 12 | −177 | −321 | −555 | −997 | |
| $10_{71}+$(o) | 9 | +3622 | +6494 | +11681 | +20912 | |
| $10_{71}+$(p) | 10 | +3924 | +7066 | +12744 | +22981 | |
| $10_{71}+$(q) | 11 | +2180 | +3908 | +7054 | +12695 | |
| $10_{71}+$(r) | 9 | +9311 | +16964 | +30879 | +56152 | |
| **$10_{71}+$** | **15(λ)** | **+61916** | **+111864** | **+202204** | **+365124** | **D** |
| $10_{81}+$(a) | 3 | 0 | 0 | 0 | 0 | |
| $10_{81}+$(b) | 8 | +56 | +98 | +172 | +302 | |
| $10_{81}+$(c) | 5 | −66 | −113 | −204 | −365 | |
| $10_{81}+$(d) | 4 | 0 | 0 | 0 | 0 | |
| **$10_{81}+$** | **8(λ)** | **−10** | **−15** | **−32** | **−63** | **L** |

[a] For each knot, the line corresponding to $\sum w'_{\lambda}, \sum w'_{\lambda+1}, \ldots$ is indicated in boldface.

The proof of this theorem parallels that of eq. (4) in [1].

Any vertex-bicolored digraph of a link is regular of degree two. It follows that all $w'_p$'s should be zero for all oriented links with $w'_0(D'_{min}) = 0$. In order to break this regularity, the distinction between parallel double arcs and single arcs is ignored in our method. The vertex-bicolored digraphs corresponding to all $D'_{min}$'s of the two oriented knots $10_{88}+$ and $10_{115}+$ are regular but do not contain any parallel double arcs. All of their $w'_p$'s are therefore unavoidably zero.

## 3. Non-oriented links and knots

Orientation of a given non-oriented chiral link may result in oriented links with

different linking numbers; for example, $7_5^2++$ and $7_5^2+-$ have linking numbers $+2$ and $-2$. On the other hand, the sign and magnitude of the self-writhe are independent of orientation. Any two minimal-crossing diagrams of an oriented alternating link therefore have the same value of $s(D'_{min})$, and this value can be used to assign D and L configurations to non-oriented chiral alternating links or knots: a non-oriented link or knot is denoted D if $s(D'_{min}) > 0$ and L if $s(D'_{min}) < 0$. For example, $s(D'_{min})$ is $+3$ for both $7_5^2++$ and $7_5^2+-$, and non-oriented $7_5^2$ is therefore assigned the D configuration. Where the linking number is zero, as in some links (e.g., $5_1^2$) and all knots, $s(D'_{min}) = w(D'_{min})$ (eq. (1)). It follows that in those cases the configuration is simply given by the writhe, $w(D'_{min})$. Furthermore, the configuration is the same as for the corresponding oriented knot or link. For example, the non-oriented link $5_1^2$ in Fig. 1 and the knot $3_1$ in Rolfsen's tabulation [9] both have L configurations.

The use of $w(D'_{min})$ in the assignment of configurations to non-oriented knots has some precedents. In 1963, Tauber proposed that the absolute configuration of a knot be designated $R$ if $w(D'_{min}) > 0$ and $S$ if $w(D'_{min}) < 0$ [14], and asserted that "For certain knots $\sum \epsilon$ [i.e., $w(D'_{min})$] $= 0$. This is exactly as it should be, for precisely these knots are identical with their mirror images". In 1985, Walba [15] reported a convention for the specification of chirality in knots that was in all essential respects the same as Tauber's, with $\epsilon = \delta$ and $\lambda$, instead of $+1$ and $-1$, and chirality descriptors $\Delta$ and $\Lambda$, instead of $R$ and $S$. According to Walba, "The number of $\delta$'s and $\lambda$' s are then summed arithmetically. If there are the same number of $\delta$ and $\lambda$ crossings, then the knot must be topologically achiral. If there are more $\lambda$ crossings, the knot has configuration $\Lambda$. If there are more $\delta$ crossings, the knot is $\Delta$".

The Tauber–Walba scheme cannot be generally applied to non-alternating knots because the $D_{min}$'s of amphicheiral non-alternating knots do not necessarily have an equal number of over- and undercrossings. In such a case, $w(D'_{min})$ cannot be zero. For example, Thistlethwaite has found a 15-crossing non-alternating knot that is amphicheiral (Fig. 13) [16]. A far more serious flaw in the Tauber–Walba scheme is the fact that a writhe of zero is a necessary but not a sufficient condition for the amphicheirality of alternating knots [1]. Thus, the conjecture that a knot must be topologically achiral if there are the same number of $\delta$ (or $+$) and $\lambda$ (or $-$) crossings is easily refuted: there are plenty of knots with writhe zero that are topologically chiral. The simplest of these is $8_4$. Nineteen of the 32 10-crossing prime knots with writhe zero are chiral, and 13 of these are alternating [9]. Two hundred sixty-two of the 320 12-crossing prime knots with writhe zero are chiral, and 159 of these are alternating [16]. According to the Tauber–Walba scheme, all of these knots would be erroneously classified as amphicheiral. As noted above, a writhe of zero may not even be a *necessary* condition for non-alternating amphicheiral knots. As a further example, the product knot $P_1 \# P_2^*$ composed of a Perko pair with $w(P_1) = +10$ and $w(P_2^*) = -8$ has writhe $+2$ even though it is topologically achiral. This knot can be isotoped to its mirror image, $P_1^* \# P_2$, with writhe $-2$, or to composite knots $P_1 \# P_1^*$ and $P_2 \# P_2^*$, both with writhe zero [1]. The method of writhe pro-

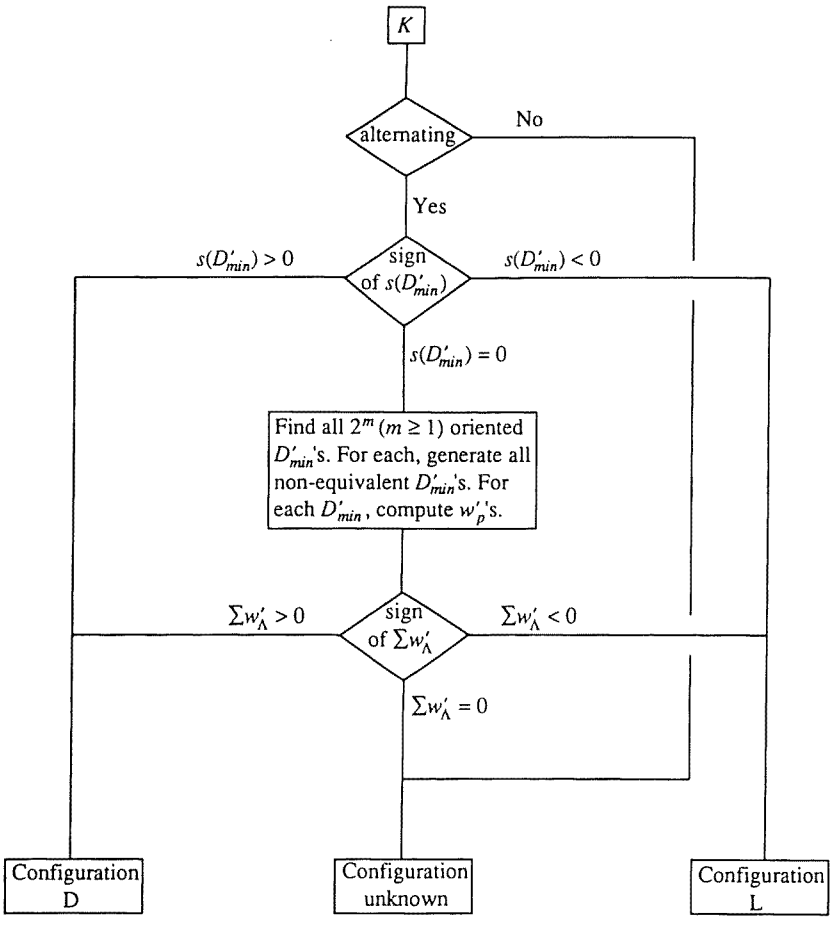


Fig. 12. Flowchart for the D/L specification of a given non-oriented chiral link or knot $K$.

files [1] was developed principally in order to find a way of assigning configurations to chiral knots *including* those with writhe zero. The present approach (see flowchart in Fig. 12), though substantially modified from [1], retains the concept of writhe profiles.

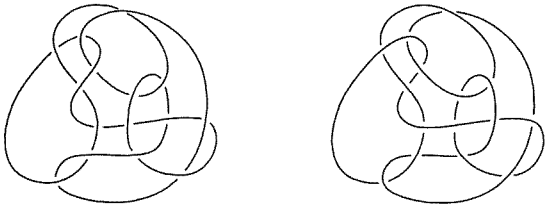

Fig. 13. Minimal-crossing diagrams of the *same* 15-crossing amphicheiral non-alternating knot with oppositely signed writhes, $w(D'_{min}) = -1$ (left) and $w(D'_{min}) = +1$ (right) [16].

The assignment of configurations to alternating knots and links with $s(D'_{min}) = 0$ is less straightforward than for those with $s(D'_{min}) \neq 0$. The first step is the generation of all $2^m$ oriented $D'_{min}$'s that correspond to a given non-oriented link or knot $K$ and the $n_{neq}(K')$ diagrams of each. Next, writhe profiles are calculated for all of these oriented diagrams. The profiles are then added, after determining the largest $p_{min}$ among the summands, as described in the preceding section for oriented links and knots. The configuration, D or L, of the non-oriented link or knot is determined by the sign of the first nonzero member of the series, $\sum w'_\Lambda$: D if $\sum w'_\Lambda$ is positive and L if it is negative. Results for $4_1^2$ (Fig. 3), $8_{10}^2$ (Fig. 9), and for ten other prime links with up to nine crossings and four components (Fig. 14) are summarized in Table 4. Note that the oriented links $4_1^2 + -$, $6_1^2 + -$, and $8_1^2 + -$ are regular but do not contain any parallel double arcs; according to eq. (7), all of the $w'_p$'s in each link are therefore equal to $w'_0$ (see Table 4).

Writhe profiles and configurations of the 14 non-oriented chiral alternating prime knots with up to 10 crossings and $w(D'_{min}) = 0$ had previously been reported in Table 14 of [1]. With three exceptions, the configurations determined by the present method are the same as those reported earlier. The three exceptions are $8_4$, $10_{93}$, and $10_{108}$, whose configurations are now D, D, and L, respectively, instead of L, L, and D.

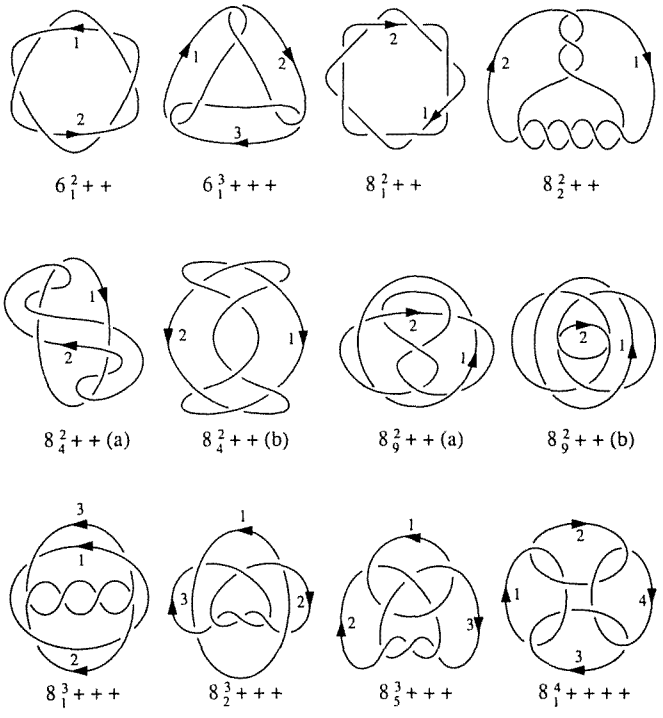


Fig. 14. Minimal-crossing diagrams of non-oriented chiral alternating links with zero self-writhe. Labeling and orientation of components follow the convention in [4].

Table 4
Writhe profiles and configurations of all non-oriented chiral alternating prime links with up to 9 crossings and 4 components, and with $s(D'_{min}) = 0$ [a].

| Link diagram [b] | $p_{min}$ | $w'_{\lambda}$ | $w'_{\lambda+1}$ | $w'_{\lambda+2}$ | $w'_{\lambda+3}$ | D/L |
|---|---|---|---|---|---|---|
| $4_1^2 + +/- -$ | 0 | +4 | +8 | +16 | +32 | |
| $4_1^2 + -/- +$ | 0 | −4 | −4 | −4 | −4 | |
| **$4_1^2$** | **0**(λ) | **0** | **+8** | **+24** | **+56** | **D** |
| $6_1^2 + +/- -$ | 0 | +6 | +12 | +24 | +48 | |
| $6_1^2 + -/- +$ | 0 | −6 | −6 | −6 | −6 | |
| **$6_1^2$** | **0**(λ) | **0** | **+12** | **+36** | **+84** | **D** |
| $6_1^3 + + + /- - -$ | 0 | +12 | +24 | +48 | +96 | |
| $6_1^3 + + -/+ -+/+ - -/- ++/- +-/- - -$ | 1 | −2 | −4 | −6 | −10 | |
| **$6_1^3$** | **1**(λ) | **+12** | **+24** | **+60** | **+132** | **D** |
| $8_1^2 + +/- -$ | 0 | +8 | +16 | +32 | +64 | |
| $8_1^2 + -/- +$ | 0 | −8 | −8 | −8 | −8 | |
| **$8_1^2$** | **0**(λ) | **0** | **+16** | **+48** | **+112** | **D** |
| $8_2^2 + +/- -$ | 0 | +8 | +12 | +19 | +30 | |
| $8_2^2 + -/- +$ | 0 | −8 | −14 | −25 | −44 | |
| **$8_2^2$** | **0**(λ) | **0** | **−4** | **−12** | **−28** | **L** |
| $8_4^2 + +(a)/- -(a)$ | 0 | +8 | +16 | +32 | +64 | |
| $8_4^2 + +(b)/- -(b)$ | 0 | +8 | +15 | +28 | +52 | |
| $8_4^2 + -(a)/- +(a)$ | 0 | −8 | −12 | −18 | −24 | |
| $8_4^2 + -(b)/- +(b)$ | 0 | −8 | −12 | −18 | −26 | |
| **$8_4^2$** | **0**(λ) | **0** | **+14** | **+48** | **+132** | **D** |
| $8_9^2 + +(a)/- -(a)$ | 1 | +8 | +16 | +32 | +64 | |
| $8_9^2 + +(b)/- -(b)$ | 1 | +8 | +16 | +32 | +64 | |
| $8_9^2 + -(a)/- +(a)$ | 1 | −6 | −10 | −18 | −31 | |

| | | | | | | |
|---|---|---|---|---|---|---|
| $8_9^2$ + −(b)/−+(b) | 1 | −6 | −12 | −18 | −34 | |
| **$8_9^2$** | **1(λ)** | **+8** | **+20** | **+56** | **+126** | **D** |
| $8_{10}^2$ + +(a)/−−(c)/+−(d)/−+(b) | 7 | +1475 | +2720 | +5025 | +9280 | |
| $8_{10}^2$ + +(b)/−−(d)/+−(c)/−+(a) | 5 | +1866 | +3460 | +6410 | +11884 | |
| $8_{10}^2$ + +(d)/−−(b)/+−(a)/−+(c) | 5 | +1140 | +2116 | +3920 | +7268 | |
| $8_{10}^2$ + +(c)/−−(a)/+−(b)/−+(d) | 13 | +163 | +288 | +551 | +1008 | |
| **$8_{10}^2$** | **13(λ)** | **+18576** | **+34336** | **+63624** | **+117760** | **D** |
| $8_1^3$ + + + / + − − / − + + / − −− | 1 | −14 | −21 | −32 | −46 | |
| $8_1^3$ + + − / − −+ | 0 | +128 | +256 | +512 | +1024 | |
| $8_1^3$ + − + / − +− | 4 | +18 | +34 | +62 | +110 | |
| **$8_1^3$** | **4(λ)** | **+236** | **+496** | **+1020** | **+2084** | **D** |
| $8_2^3$ + + + / − −− | 0 | +115220 | +202197 | +354831 | +622685 | |
| $8_2^3$ + + − / − +− [c] | 1 | −145524 | −269740 | −499976 | −926740 | |
| $8_2^3$ + − + / − −+ [c] | 1 | −145524 | −269740 | −499976 | −926740 | |
| $8_2^3$ + − − / − ++ | 17 | −21 | −30 | −39 | −52 | |
| **$8_2^3$** | **17(λ)** | **−933794** | **−1753586** | **−3290224** | **−6168654** | **L** |
| $8_5^3$ + + + / + − − / − + + / − −− | 11 | −102 | −146 | −217 | −345 | |
| $8_5^3$ + + − / + − + / − + − / − −+ | 1 | +4096 | +8192 | +16384 | +32768 | |
| **$8_5^3$** | **11(λ)** | **+15976** | **+32184** | **+64668** | **+129692** | **D** |
| $8_1^4$ + + + +/ − − − − | 0 | +2048 | +4096 | +8192 | +16384 | |
| $8_1^4$ + + + −/ + + − +/ + − + +/ + − − −/ − + + + / − + − −/ − − + −/ − − − + | 2 | +108 | +162 | +324 | +486 | |
| $8_1^4$ + + − −/ + − + −/ − + − +/ − − + + | 8 | +20 | +28 | +52 | +92 | |
| $8_1^4$ + − − +/ − + + − | 0 | −128 | −192 | −256 | −384 | |
| **$8_1^4$** | **8(λ)** | **+4784** | **+9216** | **+18672** | **+36256** | **D** |

[a] See Table 1, footnote (a).

[b] When the diagrams of several orientations are equivalent, their names are separated by a "slash" symbol and their writhe profiles are listed on a single line.

[c] By flypes, $8_2^3$ + + − / − +− and $8_2^3$ + − + / − −+ each generate two more non-equivalent diagrams that are the same as $8_2^3$ − − + / + −+ and $8_2^3$ − + − / + +−, respectively. The numbers in the two lines must therefore be multiplied by 4 instead of 2.

## 4. Can knots and links be partitioned into homochirality classes?

Although the purpose of our scheme is purely pragmatic, the question naturally arises whether knots and links that belong to the same configurational descriptor class, D or L, also share a common topological feature. If this were the case, attribution of D and L configurations would then acquire a deeper significance, and it would make sense to place topologically chiral knots and links into "right-handed" and "left-handed" homochirality classes. Any two knots or links in each class would then be "homochirally similar" [17, 18], in the manner of "two equal and similar right hands" [17]. But is this deeper meaning justified? More specifically, are the crucial requirements for an acceptable division between right- and left-handed objects satisfied?

Objects in homochirality classes [18, 19] must satisfy five conditions. First, every chiral member of an "object class" (e.g., helices) is either in a "right-handed" (**R**) or in a "left-handed" (**L**) configuration space. Second, every chiral object in **R** is matched by its enantiomorph in **L**. Third, if achiral members exist within the object class, they are neither in **R** nor in **L**. Fourth, if enantiomorphous objects can be interconverted by continuous deformation, such an interconversion can take place only by way of an achiral intermediate. Fifth, objects within each configuration space are "chirally connected", in the sense that they can be rendered congruent by continuous deformation along chiral pathways. Such objects are said to be "homochirally similar". As an example from geometry [19], consider the set of triangles in Euclidean 2-space ($E^2$). Scalene triangles are chiral in $E^2$, and the enantiomorphs are characterized by the orientation, clockwise (**R**) vs. anticlockwise (**L**), of the sides arranged in the order largest ($l$) > medium ($m$) > smallest ($s$). Enantiomorphous triangles are represented as points in a pair of two-dimensional configuration spaces that are separated by a one-dimensional boundary; the points that make up this boundary space represent achiral triangles. There is no constraint on the shape of the individual scalene triangles so long as they share the same chiral characteristic, **R** or **L**. Homochirally similar triangles may be interconverted by continuous deformation in $E^2$ and are therefore chirally connected, whereas conversion of any given scalene triangle into its enantiomorph by continuous deformation in $E^2$ inevitably requires a route along an achiral pathway that leads through an achiral (in $E^2$) isosceles or equilateral triangle. That is, passage between the **R** and **L** spaces is impossible without crossing an achiral boundary.

The enantiomorphs of a chiral knot or link cannot be interconverted by continuous deformation in $E^3$. On the other hand, the geometrically different presentations of each individual enantiomorph *can* be interconverted by continuous deformation in $E^3$ and are therefore homochirally similar. The presentations of each chiral knot or link thus fall into two homochirality classes, D and L, as illustrated in Fig. 15 for the enantiomorphs of the trefoil knot. The situation is analogous to one encountered in chemistry, where the conformations (i.e., various geometric shapes that result from bond angle deformations, bond stretching, and bond torsion) of a given

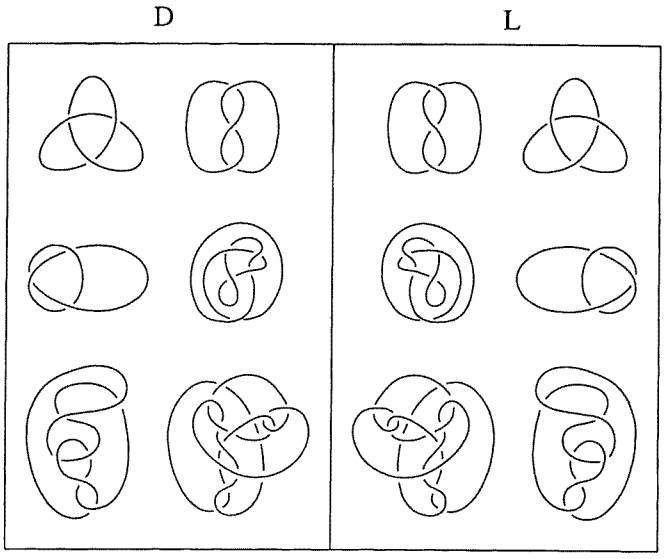


Fig. 15. Diagrams of the enantiomorphous trefoil knots, $3_1$ and $3_1^*$. Left: Homochiral presentations for the D-configuration ($3_1^*$). Right: Homochiral presentations for the L-configuration ($3_1$).

chiral molecule are partitioned into two homochirality classes, denoted *R* and *S*, Δ and Λ, etc.

In contrast, different knots and links with, say, D configurations are not homochirally similar because their presentations cannot be rendered congruent by continuous deformation in $E^3$. Thus, no general commonality, other than of a common configurational descriptor, can be claimed for the different links and knots within each (D or L) configuration space, just as different chiral molecules that have in common only their configurational descriptor, for example (*S*)-$CHClBrCH_3$ and (*S*)-alanine, are otherwise chemically distinct. The failure of the homochirality con-

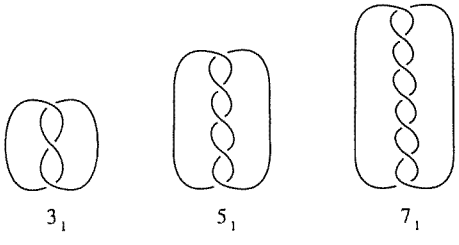


Fig. 16. Minimal-crossing diagrams of presentations with $D_2$ symmetry for the L-configuration of knots $3_1$, $5_1$, and $7_1$.

cept in this crucial respect answers the question posed above: no deeper meaning can be attached to our D/L classification of links and knots.

Nevertheless, knots or links may be grouped into configurational families, like the family of L-$\alpha$-amino acids in chemistry, that have in common some structural characteristic, even though the members of such families are not homochirally similar. As an example, members of the family of knots $3_1, 5_1, 7_1, \ldots$ are characterized by a double helix along one of the $C_2$ axes of the $D_2$ presentation; the sense of the double helix is left-handed for the L-configuration (Fig. 16) and right-handed for the D-configuration.

## Acknowledgements

Support by the National Science Foundation is gratefully acknowledged. C.C. thanks the National Fund for Scientific Research (Belgium) for partial financial support.

## References

[1] C. Liang and K. Mislow, J. Math. Chem. 15 (1994) 35.
[2] C. Liang and K. Mislow, J. Math. Chem. 18 (1995) 1.
[3] A. Kawauchi, Proc. Jap. Acad. 55, Ser.A (1979) 399;
R.H. Fox, A quick trip through knot theory, in: *Topology of 3-Manifolds*, ed. M.K. Fort, Jr. (Prentice Hall, Englewood Cliffs NJ, 1962) pp. 120–167;
R.H. Crowell and R.H. Fox, *Introduction to Knot Theory* (Blaisdell, New York, 1963).
[4] H. Doll and J. Hoste, Math. Comput. 57 (1991) 747. For a depiction of the diagrams, see Appendix A of the microfiche supplement, pp A-1 to A-10.
[5] C.C. Adams, *The Knot Book: An Elementary Introduction to the Mathematical Theory of Knots* (Freeman, New York, 1994) pp. 16–22.
[6] C.K. Murasugi, Math. Proc. Cambridge Philos. Soc. 102 (1987) 317;
L. Kauffman, Topology 26 (1987) 395;
M.B. Thistlethwaite, Topology 27 (1988) 311.
[7] E. Flapan, Topological techniques to detect chirality, in: *New Developments in Molecular Chirality*, ed. P.G. Mezey (Kluwer Acad. Publ., Dordrecht, 1991) pp. 209–239.
[8] L.H. Kauffman, Trans. Amer. Math. Soc. 318 (1990) 417.
[9] D. Rolfsen, *Knots and Links* (Publish or Perish, Berkeley, 1976; second printing with corrections: Publish or Perish, Houston, 1990), Appendix C: Table of knots and links, pp. 388–429.
[10] P.G. Tait, Trans. Roy. Soc. Edin. 28 (1876-77) 145–190.
[11] M.B. Thistlethwaite, Knot tabulations and related topics, in: *Aspects of Topology*, London Math. Soc. Lecture Note Series No. 93, eds. I.M. James and E.H. Kronheimer (Cambridge University Press, Cambridge, 1985) pp. 1–76.
[12] W.W. Menasco and M.B. Thistlethwaite, Bull. Amer. Math. Soc. 25 (1991) 403.
[13] R.J. Wilson, *Introduction to Graph Theory* (Wiley, New York, 1985) p. 107.
[14] S.J. Tauber, J. Res. Nat. Bur. Stand. 67A (1963) 591.
[15] D.M. Walba, Tetrahedron 41 (1985) 3161.

[16] M.B. Thistlethwaite, personal communication.
[17] W.T. Kelvin, The Second Robert Boyle Lecture, J. Oxford Univ. Junior Scientific Club 18 (1894) 25;
W.T. Kelvin, *Baltimore Lectures on Molecular Dynamics and the Wave Theory of Light* (C.J. Clay, London, 1904) p. 619.
[18] E. Ruch, Theor. Chim. Acta (Berl.) 11 (1968) 183;
E. Ruch, Acc. Chem. Res. 5 (1972) 49.
[19] K. Mislow, Fuzzy restrictions and inherent uncertainties in chirality studies, in: *Fuzzy Logic in Chemistry*, ed. D.H. Rouvray (Academic Press, New York, in press).